



**Flexible interdigital-electrodes based triboelectric generators for harvesting sliding and rotating mechanical energy**

Journal:	<i>Journal of Materials Chemistry A</i>
Manuscript ID:	TA-ART-08-2014-004137.R1
Article Type:	Paper
Date Submitted by the Author:	20-Sep-2014
Complete List of Authors:	Leng, Qiang; Chongqing University, Applied Physics Guo, Hengyu; Chongqing University, Applied Physics He, Xianming; Chongqing University, Applied Physics Liu, Guanlin; Chongqing University, Applied Physics Kang, Yue; Chongqing University, Applied Physics Hu, Chenguo; Chongqing University, Applied Physics Xi, Y; Chongqing University, Applied Physics

## PAPER

**Flexible interdigital-electrodes based triboelectric generators for harvesting sliding and rotating mechanical energy**

Cite this: DOI:  
10.1039/x0xx00000x

Qiang Leng<sup>†</sup>, Hengyu Guo<sup>†</sup>, Xianming He, Guanlin Liu, Yue Kang, Chenguo Hu\*, Yi Xi\*

Received 00th xxx 2014,  
Accepted 00th xxx 2014

DOI: 10.1039/x0xx00000x

www.rsc.org

Triboelectric generators have attracted great attention due to their rapidly improved electromechanical conversion efficiency. It is a great challenge to design a triboelectric generator to realize practical and effective operations. In this paper, we present a flexible interdigital-electrodes based triboelectric generator (FITG) for harvesting sliding and rotating mechanical energy. When the film of flexible interdigital-electrodes is placed on a plane, it can be used for harvesting sliding energy. When the film of the flexible interdigital-electrodes is rolled into cylinder, it can be used for harvesting rotating energy. In sliding mode, the maximum open-circuit voltage, short-circuit current and peak power density reach up to 400 V, 120  $\mu\text{A}$  (10  $\text{mA}/\text{m}^2$ ) and 13  $\text{W}/\text{m}^2$ , respectively, under sliding velocity of 3.95 m/s, which can be used to light tens of light-emitting diodes (LEDs) and to charge a commercial capacitor to 7.2 V within 35 s. The FITG can harvest mechanical energy of the mouse operation and traditional printing. In rotating mode, the maximum output voltage of the generator reaches as high as 1020 V at the rotating speed of 240 r/min. The FITG with interdigital-electrodes on flexible substrate has advantages of light weight, resistance to wear, multifunction and high output power.

**Introduction**

With the pursuit of high-quality life and the rapid development of human society, energy is playing an increasingly important role in people's life. As fossil energy is gradually being used up, it is urgent to search for green, renewable and sustainable energy resources. Harvesting energy from our ambient environment has attracted increasing attention for its extensive application in self-powered systems and small-scale energy needs.<sup>1-3</sup> In the past decade, various approaches for scavenging energy by using photovoltaic,<sup>4-6</sup> thermoelectric,<sup>7-9</sup> piezoelectric,<sup>10-12</sup> and triboelectric effects<sup>13-17</sup> have been widely investigated. Currently, the triboelectric nanogenerator based on electrification and electrostatic induction effect is considered as one of the most promising methods because it can harvest almost any random mechanical energy including airflow,<sup>18,19</sup> vibration<sup>20,21</sup> and human motion.<sup>22,23</sup> To generate electricity, two triboelectric layers with opposite charges are made to contact and separate from each other under external mechanical motion.<sup>24</sup> Recently, a TENG with two stationary electrodes and one freestanding triboelectric layer that moves in between under the guidance of external mechanical motion is developed. Furthermore, the electrode on the sliding part has been removed in a new design and a dielectric polymer layer can be inserted between the sliding part and stationary electrodes, with which the TENG can largely increase its lifetime and its energy conversion efficiency.<sup>25-27</sup> With a

free standing sliding part, this kind of triboelectric generator can avoid the entanglement of the conducting wires connected on the electrodes when it works.

In previous literatures,<sup>24,28</sup> the output of the TENG is strictly associated with the effective periodic switching between charge contact and separation. If the switching interval could be greatly shortened, the output performance of the TENG would be markedly promoted. Most of the previous generators are based on rigid electrodes, which make them not be easily assembled into device system and realize multifunction. Therefore, the generators based on flexible electrodes are needed to meet the requirement of the self-powered electronic systems. In this paper, we design a flexible interdigital-electrode based triboelectric generator (FITG) in which numerous stationary interdigital electrodes are fabricated on a flexible polyvinyl chloride (PVC) film that can be bended or folded at any angles and in any shapes. As for each of the Al electrodes, several fingers connected in one are aligned in parallel. The FITG can work in two modes, one is in sliding mode, and the other is in rotating mode. For sliding mode, the film of flexible interdigital-electrodes is flatly overlapped by one freestanding sliding panel with PTFE stripes on it, and between the film of electrodes and sliding panel sandwiched with a polyethylene terephthalate (PET) thin film. For rotating mode, the film of flexible interdigital-electrodes is rolled into a cylinder and PTFE stripes on another cylinder is put inside the electrode cylinder, and between these coaxial cylinders

also sandwiched with a PET thin film. The performance of the generator under different conditions, such as, with different numbers of strips, at different sliding/rotating speeds, by different pressure on the sliding panel, with different thickness and type of the sandwiched dielectric layer, are investigated. In sliding mode, the maximum open-circuit voltage, short-circuit current and peak power density reach up to 400 V, 120  $\mu\text{A}$  and 13  $\text{W}/\text{m}^2$ , respectively, which is used to light tens of light-emitting diodes (LEDs) and to charge a commercial capacitor to 7.2 V within 35 s. The FITG can harvest mechanical energy of the mouse operation and traditional printing. In rotating mode, the maximum output voltage of the generator reaches 1020 V at the rotating speed of 240 r/min. The FITG with interdigital-electrodes on flexible substrate has advantages of light weight, resistance to wear, multifunction and high output power.

## Experimental Section

### Fabrication of FITG for sliding mode

The structure of FITG for sliding mode is shown in **Figure 1a**, which illustrates two parts, the electrode part and sliding part. **Figure 1c** exhibits a digital photograph of FITG, demonstrating that the electrode part is flexible which can be bent into a cambered surface or rolled into a cylinder. The following is the fabrication methods of each part.

**Electrode part:** the electrode part is like a sandwich structure. In this experiment, a piece of commercial aluminium foil (width: 10 cm, length: 20 cm, thickness: 100  $\mu\text{m}$ ) was stuck on a piece of PVC film (width: 10 cm, length: 25 cm, thickness: 50  $\mu\text{m}$ ) for interdigital electrode fabrication. In the cutting process, the aluminium foil was carefully patterned to the interdigital electrodes (width of each electrode: 3 mm, interval between two electrodes: 1 mm) (**Figure 1a**). After the cutting step, a PET or PVC film with various thicknesses (from 12.5  $\mu\text{m}$  to 75  $\mu\text{m}$ ) was covered on the surface of the electrodes for comparative experiments.

**Sliding part:** the sliding part contains several PTFE strips (with surface inductively coupled plasma reactive ion etching treatment) (**Figure 1b**) as electret material (100  $\mu\text{m}$ ) and an acrylic plate (thickness: 2 mm) as a substrate. The PTFE was cut into 3 mm in width and 4 cm in length for each piece, and stuck to an acrylic panel in parallel rows with an interval of 5 mm (**Figure 1c**). The number of the strips varies from 1 to 15.

### Fabrication of FITG for rotating mode

**Electrode part:** The sizes of the electrode film and electrode strips are 8 cm $\times$ 8.5 cm and 5 mm $\times$ 6 mm, respectively. The electrode film is rolled and attached onto the inside wall of the glass cylinder with a PET film covering its exposure surface as shown in **Figure 1d**.

**Rotating part:** Ten PTFE strips are stuck on the outside wall of another glass cylinder with a gap of 7 mm between two adjacent ones as is shown in **Figure 1d**. The PTFE strip is cut into 5 mm in width and 6 cm in length. The rotating part is inserted into the outer cylinder as is depicted in **Figure 1e** and **1f**.

### Characterization of FITG

The output performance of FITGs was measured using a Stanford low-noise current preamplifier (Model SR570) and a Data Acquisition Card (NI PCI-6259). In sliding mode, the electrode part was fixed on a plate, while a linear motor (42HBS48BJ4-TR0) and a governor (ZD-6209-V2(C)) were used to form a motion with

different frequency on the sliding part with various weights on it, so that we can study the influence of speed and pressure on output performance. **Figure S1** schematically shows the measuring system.

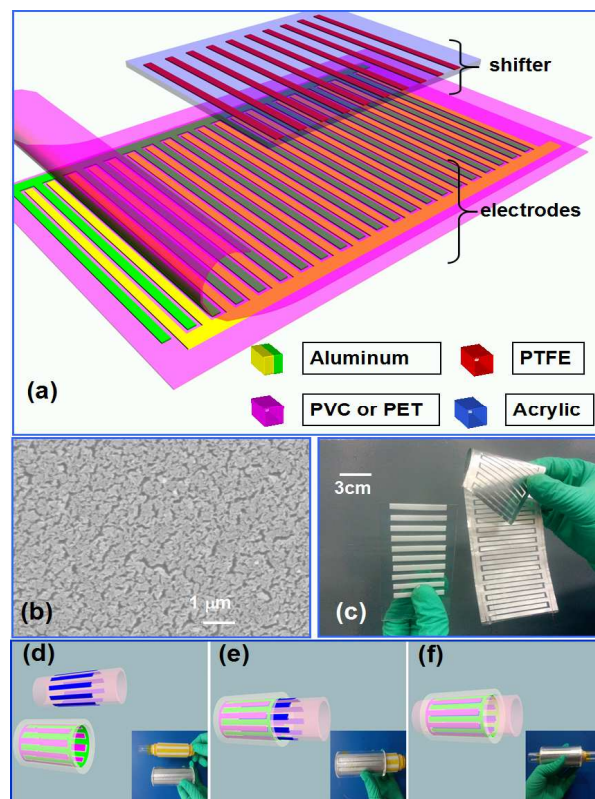


**Figure 1.** (a) The schematic diagram of the FITG structure for sliding mode, including the sliding part and electrode part. (b) SEM image of the PTFE surface. (c) A digital photograph of FITG for sliding mode. (d)–(f) Schematic diagram of the fabrication of the FITG for rotating mode. The insets are the corresponding digital photographs of real device in preparation steps.

In rotating mode, the electrode cylinder was fixed while the PTFE cylinder was driven to rotate by an electrical motor (51K40RA-D1500) with a digital display speed controller. The software Comsol Multiphysics based on finite-element simulation was employed to simulate the potential distribution in the FITG under open circuit condition.

## Results and discussion

### Interdigital electrode structure

Each yellow or green electrode is connected in one end respectively to form interdigital electrodes as is shown in **Figure 1a**. The surface of the PTFE strips treated by ion etching is shown in **Figure 1b**. The interdigital electrodes are quite flexible as is exhibited in **Figure 1c**, which can be folded in any shapes. Moreover, this structure leads to excellent reliability and durability because the metal electrodes covered with PET/PVC thin film are not directly rubbed by the sliding panel.

### Electricity generation process in sliding mode

The electricity produced by TENGs originates from the mechanical motion through the coupling of triboelectrification and electrostatic induction: the periodic contact and separation between two different medium with opposite charges change the induced potential

difference across the two electrodes and thereby drive the alternating flow of electrons through an external load.<sup>29-31</sup> Figure 2 presents the electricity generation process in sliding mode in detail. Figure 2(a) shows the output current change during a whole sliding cycle. Because of the large difference in the ability to obtain electrons, after being rubbed by each other, the PVC surface has positive charges and the PTFE has negative charges (See Figure 2(b1)).<sup>32</sup> We define the initial state (Figure 2(b1) and Figure 2(f1)) or the final state (Figure 2(d1)) when the electrode A (green) or electrode B (yellow) is overlapped by the PTFE strip. Figure 2(c1) and 2(e1) represent the middle states where the sliding panel moves between the initial state and the final state.

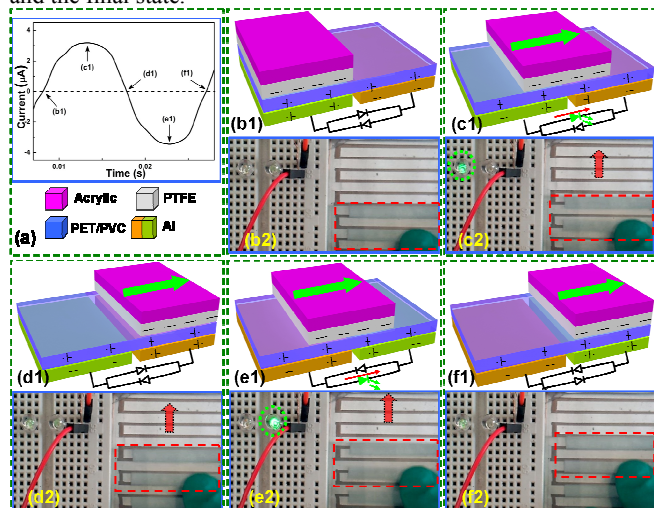


**Figure 2.** Working mechanism of FITG for sliding mode. (a) The output current in a sliding cycle, (b1) the electrode A is overlapped by one PTFE strip, (c1) the sliding panel moves from electrode A to B, (d1) the electrode B is overlapped by PTFE, (e1) the sliding panel slides away from electrode B to A. (f1) Initial state after a sliding cycle. (b2–f2)

To analyze the electricity generating process, two light-emitting diodes (LEDs) are connected with the FITG. At the initial state, induced charges appear on electrode A (positive) and electrode B (negative) with equal charge density as is illustrated in Figure 2(b1). Without electron transfer, no current flows in the circuit, which can be evidenced by the unlighted LEDs in Figure 2(b2). As the sliding panel moves from state in Figure 2(b1) to Figure 2(d1), the charges on the electrode surface start to transfer. Free electrons flow from electrode B to A until the PTFE is in the state (Figure 2(d1)) where the charges reach a new equilibrium. Thus, there is a current flow from electrode A to B, which can be verified by lighting the left LED as is shown in Figure 2(c2) until zero (Figure 2(d2)). As electrode A and B are alternately aligned, in the next step, the sliding panel moves from electrode B to A (Figure 2(e1)), while the free electrons flow from electrode A to electrode B until the sliding panel is in the state (Figure 2(f1)). The current flows reversely from electrode B to electrode A which drives the right LED lightening as is shown in Figure 2(e2) until zero (Figure 2(f2)). In the whole cycle, that the sliding panel moves from electrode A group to electrode B group and from electrode B group to electrode A group are symmetric, so a pair of symmetric alternating current peaks are monitored, as is depicted in Figure 2(a). The total charge transfer quantity and current can be expressed by the following equation<sup>33,34</sup>

$$Q = n \cdot \sigma \cdot l \cdot w(t) \quad 0 \leq w(t) \leq w_0 \quad (1)$$

$$I = \frac{dQ}{dt} = n \cdot \sigma \cdot l \cdot \frac{dw(t)}{dt} = n \cdot \sigma \cdot l \cdot v \quad (2)$$

Where  $n$ ,  $\sigma$ ,  $l$  and  $w_0$  are the number of the PTFE strips, the triboelectric charge density on the PTFE strips, the length and width of a single PTFE strip, and  $w(t)$  is the displacement of the strips moving away from the initial state, and  $v$  is the sliding velocity of the sliding panel. To further study the process of electricity generation, we also simulate the potential difference between the two groups of interdigital electrodes at different time or state using COSMOL Multiphysics software (Figure S2).

### Number of PTFE strips on sliding panel

The charge transfer quantity per unit time mainly determines the output current magnitude from equation (2), while the quantity of charges on an electrode depends on the charge density of the PTFE strips and total overlapped area with the electrodes from equation (1). To investigate the influence of the overlapped area on the output current, we change the number of the PTFE strips. With the increase in the number of the strips, the output current increases correspondingly, as is shown in Figure 3a. The maximum output current can reach about 12  $\mu\text{A}$  with 15 PTFE strips. As the PTFE strips are added, the area becomes larger and accordingly increases the total quantity of electric charges in accordance with equation (1). From Figure 3b, the total charge transfer quantity per second rises linearly as the number of PTFE strips increases, which consequently enlarges the output current.

### Pressure on sliding panel

The contact tightness between the PTFE strips and the PVC film might affect the performance of the FITG. Therefore, different pressure is applied on the sliding panel with 5 PTFE strips. From Figure 3c, when no pressure is put on, the output current is quite low and it is about 5 nA. After the pressure increases to 1 N, the value increases to 2.5  $\mu\text{A}$  much higher than that without pressure case. As the two triboelectric surfaces contact each other intimately with the pressure applied on, the effective contact area increases owing to the nanostructure on the PTFE surface, which results in the increase in charge density on PTFE film. However, as the pressure further increases from 2 N to 5 N, the output current seems to have achieved a saturation state. This is mainly because that the PTFE strips and the PVC film have already contacted sufficiently. Larger pressure contributes little to the friction charge increase. As we can see from Figure 3d, the charge transfer quantity increases with pressure at the beginning, then keeps nearly constant later, which matches well with the change of output current.

### Sliding velocity

The output current is proportional to the speed of the sliding panel according to equation (2). To verify the influence of the sliding speed on the output, we systematically study the relationships between the output current, charge transfer quantity and the sliding speed. We can obviously find that the output current increases with the increase in velocity, as is shown in Figure 3e. As for one PTFE strip, the charge transfer quantity per second a cycle remains unchanged (Figure 3f). However, the amount of charge transfer per unit time becomes larger as the sliding speed increases.

### Type of triboelectric layer

For the triboelectric nanogenerators, the generation of electricity is based on the friction between two kinds of materials with different tendency to gain or lose electrons in the triboelectrification process. To explore the influence of different types of the triboelectric layers on the performance of the FITG, we choose another organic material, PET film, to conduct a comparative experiment. With the same number of the PTFE strips, the output current with the PET film is larger, and the maximum value with 15 PTFE strips is 1.5 times larger than that of the PVC film, as is shown in **Figure 4a**. Under the same pressure and sliding speed, the performance of the FITG with the PET film is much better than that of the FITG with the PVC film, which can be seen from **Figure 4b** and **4c**. The maximum output current at the highest speed of 3.95 m/s almost doubles that with the PVC film. Compared with **Figure 3b**, **3d** and **3f**, the corresponding charge transfer under same condition also matches the tendency with the PVC film, as is shown in **Figure 4d–4f**. The output current increase may be attributed to the difference of the tendency to gain or lose electrons between the PVC film and the PET film. Using the PTFE and PET as the friction interface, high output power can be achieved due to the fact that PTFE has strong tendency to gain electrons (negative charge) while PET has strong tendency to lose electrons (positive charge). However, PTFE and PVC both have tendency to lose electrons (negative charge) although PTFE has more negative charge tendency than that of PVC.<sup>35</sup> Therefore, less negative charge density is achieved using PTFE and PVC as friction interface. The lower charge density on PTFE film would result in small output current based on equation (2). As the FITG with PET film can achieve larger charge density, we choose PET film in the experiment below.

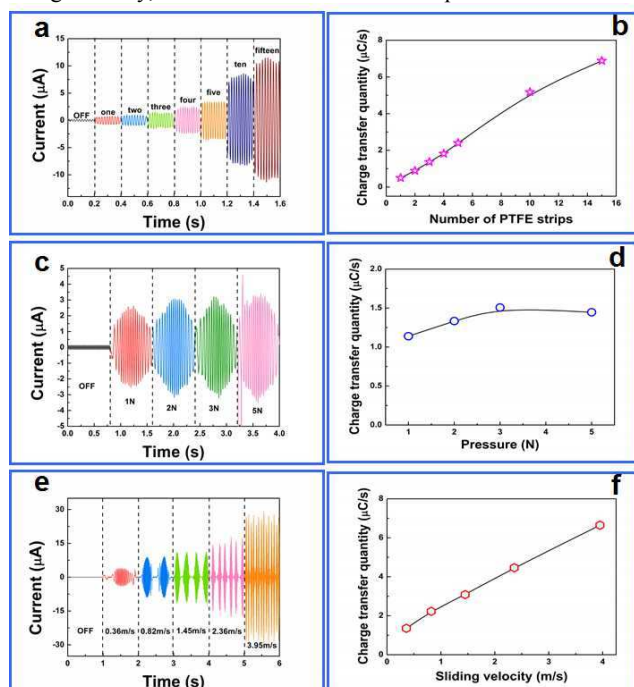


**Figure 3.** The performance of FITG with sandwiched PVC film. (a) The output current with different number of PTFE strips on the sliding panel, and (b) corresponding charge transfer quantity. (c) The output current under different pressure, and (d) corresponding charge transfer quantity. (e) The output current under different sliding speed, and (f) corresponding charge transfer quantity.

### Thickness of the triboelectric layer

To investigate whether the thickness has an influence on the performance of the FITG, the PET film with different thickness of 12.5  $\mu\text{m}$ , 25.0  $\mu\text{m}$ , 50.0  $\mu\text{m}$  and 75.0  $\mu\text{m}$  are sandwiched between the PTFE strips and the interdigital electrodes. As is shown in **Figure 5a**, with a thickness of 25.0  $\mu\text{m}$ , the output current of the FITG achieves a maximum value of about 26  $\mu\text{A}$ . However, as the thickness of the PET film increases, the output current gradually reduces to the minimum of 15  $\mu\text{A}$ . PTFE is electret and the negative charge on its surface will not change during the sliding process. Charge transfer is achieved only on the metal electrodes. As the charge transfer is driven by the electrostatic induction (electric potential difference) caused by the movement of the sliding panel, the thinner PET film would present a better driving force to the electron transfer. Therefore, it is better to choose thinner sandwiched triboelectric layer to induce efficient and rapid charge transfer between the electrodes to promote the performance of the FITG.

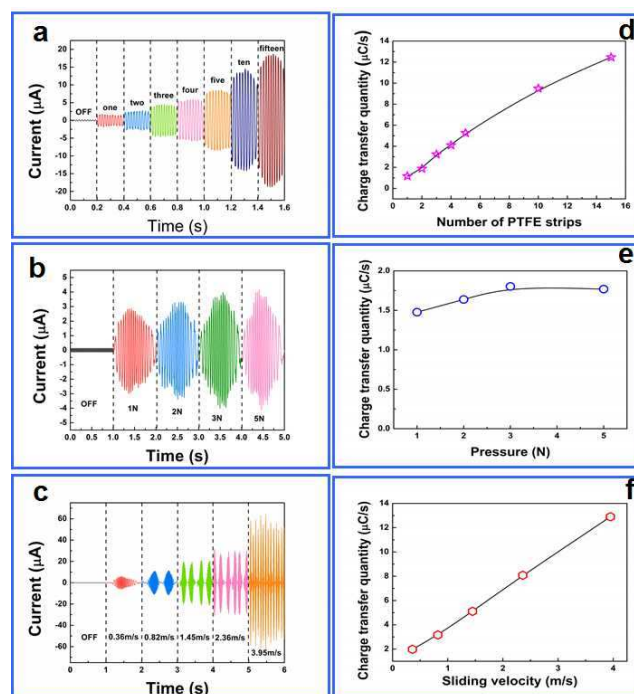


**Figure 4.** The performance of FITG with PET film. (a) The output current with different number of PTFE strips on the sliding panel, and (b) corresponding charge transfer quantity. (c) The output current under different pressure, and (d) corresponding charge transfer quantity. (e) The output current under different sliding velocity, and (f) corresponding charge transfer quantity.

To evaluate the working efficiency of the FITG working in sliding mode, investigation of the output power with different external loads is indispensable. As is displayed in **Figure 5b**, the open-circuit voltage reaches 400 V with a load resistance of 700  $\text{M}\Omega$ . **Figure S3** shows the tendency of voltage at 700  $\text{M}\Omega$ . The current amplitude drops with increase in load resistance while the voltage rises up. Consequently, the peak power reaches the maximum at a load resistance of 2  $\text{M}\Omega$  as is seen in **Figure 5c**. The output power is calculated by the following equation:

$$P=I^2R$$

The calculation of the maximum output power value is shown in Supporting Information. Moreover, to prove the endurance of the

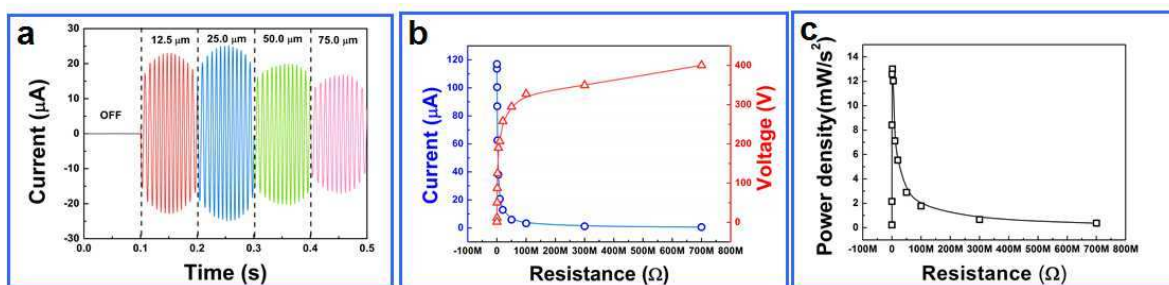


**Figure 5.** (a) The output current under different thickness of the PET film. (b) The output current and voltage under different external loads. (c) The peak power under different external loads.

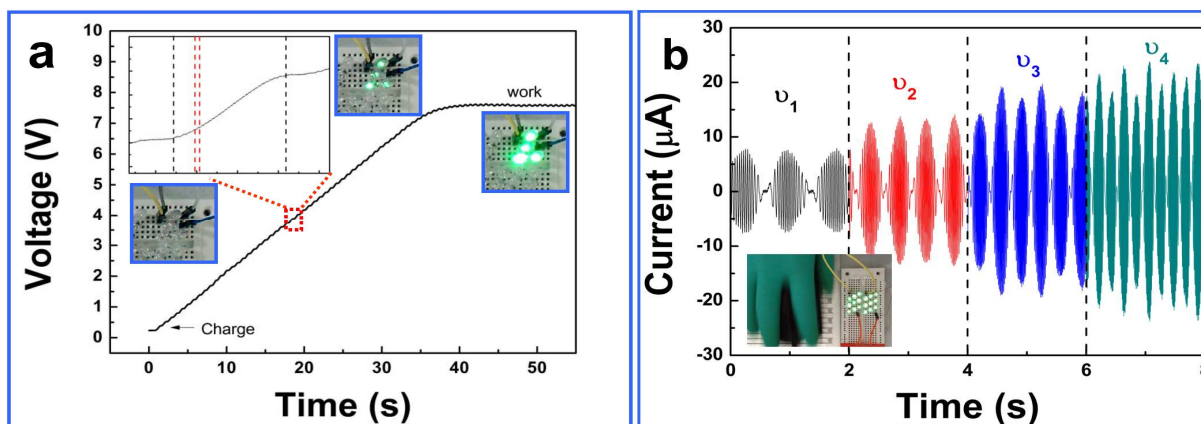


**Figure 6.** (a) The voltage charging curve of the capacitor. The left up-corner inset is the magnification of the voltage-time curve. The other three insets exhibit the whole process of charging and discharging of the capacitor. (b) The output current under different velocities of the mouse based FITG. The velocity increases from  $v_1$  to  $v_4$ .

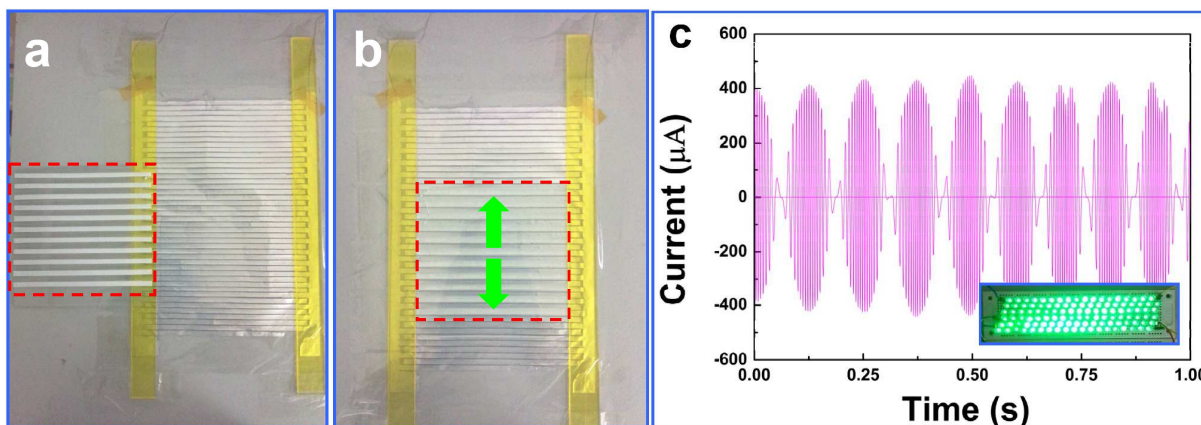


**Figure 7.** (a) (b) The structure of the traditional printing-based generator. (c) The output current of the generator. Inset is the photograph of the lit LEDs driven by the generator.

device, a test is carried out after the device is rubbed for three thousand times (See **Figure S4**).

### Charging the commercial capacitor

For tiny electronic devices, too high voltage might not be safe and this blocks the FITG from powering them directly. Therefore, an energy storage unit is necessary to convert the high voltage to a working voltage, such as a capacitor or a battery.<sup>36,37</sup> A commercial capacitor (110 μF) is chosen for charging test. Meanwhile, four light-emitting diodes (LEDs) in series are connected with the capacitor. Figure 6a shows the charging voltage-time signals, from

which we can see that the capacitor is charged from 0 V to 7.5 V within 40 s. From the inset digital photography, we can observe that the LEDs are off at the beginning due to the low electric energy charged into the capacitor. As the capacitor is charged more, the LEDs are gradually lighted until to their highest brightness. The left top-corner inset is the magnification of the voltage-time curve. The steps in the plot correspond to that the PTFE strips periodically move toward and away from electrodes. **Video 1** shows the charging and discharging of the commercial capacitor.

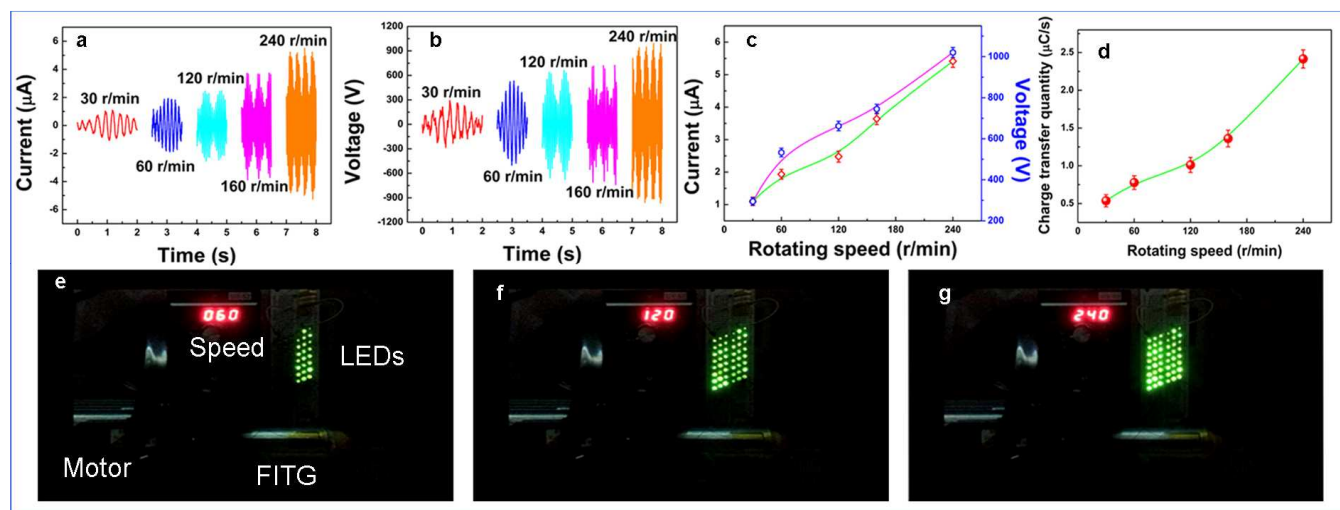


**Figure 8.** (a-d) The output current, open-circuit voltage and charge transfer quantity of the FITG working at different rotating speeds. (e-g) The digital photograph of the FITG is rotating and powering LEDs at different rotating speeds.

### Harvesting motion energy of computer mouse

Since personal computers have been popularized all around the world, and as an indispensable part, mouses move constantly. It would be attractive to utilize the energy in relative motion between the mouse and the mouse pad. Herein, our flexible interdigital electrodes act as a mouse pad. Seven strips of the PTFE are attached to the bottom of a computer mouse. As is displayed in **Figure 6b**, when we slightly move the mouse back and forth, an output current of  $\sim 5 \mu\text{A}$  is monitored. With the moving velocity accelerating, the output current increases correspondingly, which matches the results in **Figure 3c** and **4c**. Tens of LEDs can be lighted by moving the mouse, as is exhibited in the inset, implying that the simple mouse motion can generate considerable electric energy. Perhaps in the future, this mouse movement could help us to charge our electronic devices, such as mobile phone while we are working or playing. **Video 2** gives the whole working process of the mouse based FITG.

### Harvesting motion energy of traditional printing

After scaling up the sliding panel (about 4 times larger) and the interdigital electrodes (**Figure 7a**), a traditional printing-based generator is fabricated, as is shown in **Figure 7b**. Moving the sliding panel forward and backward like printing can generate quite considerable amount of electricity, which is depicted in **Figure 7c**. The maximum output current of this generator can be as high as  $\sim 0.45 \text{ mA}$ . Two rows of LEDs aligned in parallel are alternatively lit up (the inset). The brightness of these LEDs implies the high energy density output of our generator (See **Video 3**)

### FITG working in rotating mode

For a triboelectric nanogenerator, the potential capacity of scavenging different kinds of mechanical energy becomes as important as its applications. Whether the generator can be applied extensively depends on whether the device can take advantage of different energy in the ambient. To harvest rotating energy, the film of flexible interdigital-electrodes is rolled into a cylinder and PTFE stripes on another cylinder is put inside the electrode cylinder, and between these coaxial cylinders also sandwiched with a PET thin film as shown in **Figure 1d-1f**. The output current and voltage increase with the increase in the rotating speed as are shown in **Figure 8a-c**. The maximum output voltage can reach about 1020 V.

From **Figure 8d**, the charge transfer quantities per second increase with the rotating speed. The detailed calculation method of the charge transfer quantity unit time is illustrated in **Figure S5**. Through the brightness in **Figure 8d-8f** of the LEDs, the output power can be evaluated. (See **Video 4**) Both the output current and voltage can be used to determine the rotating speed.

### Conclusions

In summary, we have designed and fabricated the flexible interdigital electrodes based triboelectric nanogenerators. The interdigital electrodes help shorten the cycle of charge transfer thereby enlarge the output current. The flexibility of the interdigital electrodes makes it possible to be employed to construct generators for harvesting sliding and rotating energy. In sliding mode, the FITG generates an open-circuit voltage of 400 V and the short-circuit current of  $120 \mu\text{A}$  ( $10 \text{ mA/m}^2$ ) with a peak power of  $13 \text{ W/m}^2$  under a velocity of 3.95 m/s, which can drive tens of LEDs. The factors that influence on the output current are elaborated, among which the number of the PTFE strips and the velocity of the sliding panel are proportional to the output current while the thickness of the triboelectric layer is inversely proportional to the output current. Moreover, the larger opposite tendency to gain/lose electrons between PTFE and sandwiched film does well in achieving higher output power. The produced electrical power can be used to charge the commercial capacitor and light LEDs. The FITG can harvest mechanical energy of the mouse operation and traditional printing. In rotating mode, the maximum output voltage of the generator reaches as high as 1020 V at the rotating speed of 240 r/min. This investigation demonstrates the flexible interdigital electrodes can be used to construct multifunctional generators.

### Acknowledgements

This work is supported by the NSFCQ (cstc2012jjB0006), SRFDP (20110191110034, 20120191120039), NSFC (11204388), the Fundamental Research Funds for the Central Universities (CDJRC10300001, CDJZR11300004, CDJZR12225501, CQDXWL-2013-012).

## Notes and references

[\*] Q. Leng, H.Y. Guo, X.M. He, G.L. Liu, Prof. C.G. Hu, Prof. Y. Xi  
Department of Applied Physics, Chongqing University  
Chongqing 400044, P.R. China

E-mail: [hucg@cqu.edu.cn](mailto:hucg@cqu.edu.cn) (C. G. Hu); [yxi6@cqu.edu.cn](mailto:yxi6@cqu.edu.cn) (Y. Xi)

<sup>†</sup>These authors contributed equally to this work.

† Electronic supplementary information (ESI) available.

- 1 Y. Yang, H. L. Zhang, G. Zhu, S. Lee, Z. H. Lin, Z. L. Wang. *ACS Nano*. 2013, 7, 785-790.
- 2 P. D. Mitcheson, E. M. Yeatman, G. K. Rao, A. S. Holmes, T. C. Green. *Pro. IEEE* 2008, 96, 1457-1486.
- 3 Z. L. Wang, G. Zhu, Y. Yang, S. H. Wang, C. F. Pan. *Mater. Today* 2012, 15, 532-543.
- 4 H. Kim, H. Jeong, T. K. An, C. E. Park, K. Yong. *Appl. Mater. Interfaces* 2013, 5, 268-275.
- 5 E. G. Wang, L. T. Hou, Z. Q. Wang, S. Hellstrom, F. L. Zhang, O. Inngan, M. R. Andersson. *Adv. Mater* 2010, 22, 5240-5244.
- 6 Y. H. Chen, W. C. Lin, J. Liu, L. M. Dai. *Nano Lett.* 2014, 14, 1467-1471.
- 7 Y. Du, K. F. Cai, S. Chen, P. Cizek, T. Lin. *Appl. Mater. Interfaces* 2014, 6, 5735-5743.
- 8 D. Madan, Z. Q. Wang, A. Chen, R. C. Juang, J. Keist, P. K. Wright, J. W. Evans. *Appl. Mater. Interfaces* 2012, 4, 6117-6124.
- 9 Y. Z. Pei, A. D. LaLonde, N. A. Heinz, X. Y. Shi, S. Iwanaga, H. Wang, L. D. Chen, G. J. Snyder. *Adv Mater.* 2011, 23, 5674-5678.
- 10 Z. L. Wang, W. Z. Wu. *Ange. Chem., Int. Ed.* 2012, 51, 11700-11721.
- 11 S. Y. Xu, Y. W. Yeh, G. Poirier, M. C. McAlpine, R. A. Register, N. Yao. *Nano Lett.* 2013, 13, 2393-2398.
- 12 S. H. Shin, Y. H. Kim, M. H. Lee, J. Y. Jung, J. Nah. *ACS Nano*, 2014, 8, 2766-2773.
- 13 J. J. Cole, C. R. Barry, R. J. Knuesel, X. Y. Wang, H. O. Jacobs. 2011, 27, 7321-7329.
- 14 J. Henniker. *Nature*. 1962, 196, 474.
- 15 Y. S. Zhou, Y. Liu, G. Zhu, Z. H. Lin, C. F. Pan, Q. S. Jing, Z. L. Wang. *Nano Lett.* 2013, 13, 2771-2776.
- 16 L. S. McCarty, G. M. Whitesides. *Angew. Chem., Int. Ed.* 2008, 47, 2188-2207.
- 17 Z. H. Lin, G. Cheng, L. Lin, S. M. Lee, Z. L. Wang. *Angew. Chem., Int. Ed.* 2013, 125, 12777-12781.
- 18 C. L. Sun, J. Shi, D. J. Bayer, X. D. Wang. *Energy Environ. Sci.*, 2011, 4, 4508-4512.
- 19 Y. N. Xie, S. H. Lin, L. Wang, Q. S. Jing, Z. H. Lin, S. M. Niu, Z. Y. Wu, Z. L. Wang. *ACS Nano*. 2013, 7, 7119-7125.
- 20 W. Q. Yang, J. Chen, G. Zhu, X. N. Wen, P. Bai, Y. J. Su, Y. Lin, Z. L. Wang. *Nano Research*. 2013, 6, 880-886.
- 21 S. P. Beeby, M. J. Tudor, N. M. White. *Meas. Sci. Technol.* 17, R175.
- 22 W. Q. Yang, J. Chen, G. Zhu, J. Yang, P. Bai, Y. J. Su, Q. S. Jing, X. Cao, Z. L. Wang. *ACS Nano*. 2013, 7, 11317-11324.
- 23 P. Bai, G. Zhu, Z. H. Lin, Q. S. Jing, J. Chen, G. Zhang, J. S. Ma, Z. L. Wang. *ACS Nano*. 2013, 7, 3713-3719.
- 24 S. H. Wang, L. Lin, Z. L. Wang. *Nano Lett.* 2012, 12, 6339-6346.
- 25 S. H. Wang, Y. N. Xie, S. M. Niu, L. Lin, Z. L. Wang. *Adv Mater.* 2014, 26, 2818-2824.
- 26 L. Lin, S. H. Wang, S. M. Niu, C. Liu, Y. N. Xie, Z. L. Wang. *Appl. Mater. Interfaces*. 2014, 6, 3031-3038.
- 27 H. Y. Guo, Q. Leng, X. M. He, M. J. Wang, J. Chen, C. G. Hu, Y. Xi. *Adv. Energy. Mater.* DOI: 10.1002/aenm.201400790.
- 28 L. Lin, S. H. Wang, Y. N. Xie, Q. S. Jing, S. M. Niu, Y. F. Hu, Z. L. Wang. *Nano Lett.* 2013, 13, 2916-2923.
- 29 Y. N. Xie, S. H. Wang, L. Lin, Q. S. Jing, Z. H. Lin, S. M. Niu, Z. Y. Wu, Z. L. Wang. *ACS Nano*. 2013, 7, 7119-7125.
- 30 G. Zhu, C. F. Pan, W. X. Guo, C. Y. Chen, Y. S. Zhou, R. M. Yu, Z. L. Wang. *Nano Lett.* 2012, 12, 4960-4965.
- 31 G. Zhu, Z. H. Lin, Q. S. Jing, P. Bai, C. F. Pan, Y. Yang, Y. S. Zhou, Z. L. Wang. *Nano Lett.* 2013, 13, 847-853.
- 32 S. H. Wang, L. Lin, Y. N. Xie, Q. S. Jing, S. M. Niu, Z. L. Wang. *Nano Lett.* 2013, 13, 2226-2233.
- 33 C. Zhang, W. Tang, C. B. Han, F. R. Fan, Z. L. Wang. *Adv Mater.* 2014. DOI:10.1002/adma.201400207.
- 34 G. Zhu, J. Chen, T. J. Zhang, Q. S. Jing, Z. L. Wang, *Nature Communications*. 2014. DOI:10.1038/ncomms4426.
- 35 Z. L. Wang, *ACS Nano*. 2013, 7, 9533-9557.
- 36 H. Y. Guo, X. M. He, J. W. Zhong, Q. Z. Zhong, Q. Leng, C. G. Hu, J. Chen, L. Tian, Y. Xi, J. Zhou. *J. Mater. Chem. A* 2014, 2, 2079-2087.
- 37 Q. Z. Zhong, J. W. Zhong, B. Hu, Q. Y. Hu, J. Zhou, Z. L. Wang. *Energy Environ. Sci.* 2013, 6, 1779-1784.



## Graphical Abstract

Flexible interdigital-electrodes based triboelectric generator can harvest mechanical energy of the mouse operation and traditional printing. The generator has advantages of being flexible, light weight, durable, portable and high output power.

